

# Adaptive and integrated neighborhood-dependent approach for nonlinear enhancement of color images

Li Tao

Vijayan K. Asari

Old Dominion University

Department of Electrical and Computer Engineering  
Computational Intelligence and Machine Vision Laboratory  
Norfolk, Virginia 23529

**Abstract.** A novel image enhancement algorithm called AINDANE (adaptive and integrated neighborhood dependent approach for nonlinear enhancement) for improving the visual quality of digital images captured under extremely low or nonuniform lighting conditions is proposed. AINDANE is comprised of two separate processes, namely, adaptive luminance enhancement and adaptive contrast enhancement, to provide more flexibility and better control over image enhancement. Adaptive luminance enhancement is a global intensity transformation based on a specifically designed nonlinear transfer function, which is self-tuned by the histogram statistics of the input image. This process largely increases the luminance of darker pixels and compresses the dynamic range of the image at the same time. Adaptive contrast enhancement tunes the intensity of each pixel based on its relative magnitude with respect to the neighboring pixels. This process is also adaptively controlled by the global statistics of the image. A color restoration process, based on the relationship between the spectral bands and the luminance of the original image, is applied to convert the enhanced intensity image back to a color image. © 2005 SPIE and IS&T.  
[DOI: 10.1117/1.2136903]

## 1 Introduction

It is well known that human eyes perform much better than cameras when imaging real-world scenes, which generally produce high dynamic range radiance maps that can span more than six orders of magnitude. Currently available imaging devices can measure only about three orders of magnitude. In addition, image display devices, such as monitors and printers, also demonstrate limited dynamic range. As a result, images commonly exhibit saturation and underexposure in which some important features are eliminated or difficult to detect by human viewers. Computer vision algorithms can also have difficulty processing these images. However, the wide dynamic range radiance maps can be well handled by human eyes through a series of adaptive mechanisms for brightness perception. First, the size of pupil is variable to accommodate different levels of radiance from different regions in a scene, while the camera aperture is fixed when capturing the scene. When staring at a highly bright region in the scene, the pupil will shrink to compress the dynamic range so that the eyes can deal with it. Second, and more important, the major dynamic range compression process is taking place via the lateral processing at the reti-

nal level.<sup>1</sup> Finally, the early visual cortex is also found participating in some of the dynamic range processing.

How can we handle the high-dynamic-range scenes given the limited dynamic ranges of cameras, monitors, and printers? The answer is unique: compressing the dynamic range. Therefore, various image processing techniques have been developed to implement this concept. Some of those techniques are simple methods, such as gamma adjustment, logarithmic compression, histogram equalization, and the levels/curves methods. Those techniques generally have very limited performance: some features may be lost during the image processing, or some cannot be sufficiently enhanced. Basically, they are all based on global processing and they essentially lack local contrast enhancement to preserve or even enhance important image features or details. To obtain better performance, more advanced image enhancement techniques have been developed. These techniques are able to compress the dynamic range while maintaining or even improving local contrast to achieve high visual quality.

In this paper, a new nonlinear image enhancement algorithm called AINDANE (adaptive and integrated neighborhood dependent approach for nonlinear enhancement) is proposed to improve the visual quality of digital images captured under low or nonuniform illumination conditions. It consists of two independent processes: adaptive luminance enhancement and adaptive contrast enhancement, which are applied to treat the luminance information of images. Luminance (brightness) enhancement provides the dynamic range compression, and contrast enhancement is intended to preserve important visual details and approximate the tonality towards that of the original image. In other advanced algorithms, like the original retinex<sup>2</sup> and multiscale retinex with color restoration<sup>3</sup> (MSRCR), both processes are implemented together. The separation of the two processes provides AINDANE more flexibility and capability to tune and control the whole image enhancement process. For enhancement of color images by AINDANE, color images are first converted to intensity images prior to luminance and contrast enhancements for faster processing and consistent color rendition. The averaged luminance information of neighboring pixels, which is needed for local contrast enhancement, can be obtained using 2-D discrete convolution. To obtain better results, image enhancement techniques should be made image dependent (adaptive).

Paper 04064RR received Jun. 15, 2004; revised manuscript received Apr. 7, 2005; accepted for publication Apr. 28, 2005; published online Dec. 12, 2005.

1017-9909/2005/14(4)/043006/14/\$22.00 © 2005 SPIE and IS&T.

This requires that the image enhancement process can be tuned (controlled) by certain properties of images, such as the statistical information. After luminance and contrast enhancements have been performed, a linear color restoration process is applied to convert the intensity images back to color images using the chromatic information of the original image. Compared to other image enhancement techniques, AINDANE produces better image quality with well-balanced luminance and contrast as well as accurate and natural color rendition.

In the remainder of the paper, first, related work in image processing and computer graphics is briefly reviewed. Then we introduce the details of our algorithm. Finally, the image enhancement results are discussed and compared with those of some commonly cited techniques.

## 2 Related Work

Retinex-based algorithms are effective techniques dealing with dynamic range compression and color constancy, which are developed from Land's theory<sup>4–6</sup> of human visual perception of lightness and color. Since the introduction of retinex, several variants<sup>7–10</sup> on the original method have been developed mainly to improve the computational efficiency while preserving the basic principles. However, those methods are not widely used because of comparatively low processing speed and some issues concerning the visual quality of enhanced images. Nevertheless, more algorithms and applications have been developed based on retinex due to its deep understanding of the lightness and color perception.<sup>11,12</sup>

MSRCR (Refs. 3 and 13–16, proposed by Z. Rahman *et al.*, is a newly developed and widely cited image processing technique that is a retinex-based algorithm using logarithmic compression and spatial convolution to implement the idea of retinex. It aims to synthesizing local contrast enhancement, color constancy, and lightness/color rendition for digital color image enhancement. MSRCR generally works well with various types of images. However, it also has some drawbacks that must be tackled for approaching optimal performance.<sup>17–19</sup> Since the standard MSRCR algorithm must process all spectral bands of color images, it will take a long time to enhance large size images. Thus, MSRCR is hard to be used in real-time applications without a hardware implementation of the algorithm. In addition, the nonlinear color restoration process may produce colors that are not predictable and sometimes make images look unnatural. For images having a dark subject with a very bright background, MSRCR seems to have difficulty providing sufficient luminance enhancement for the subject without postenhancement treatment, and MSRCR may also cause the decrease in the luminance of the background, which can deteriorate the quality of the enhanced images if no posttreatment is performed. Finally, images enhanced by MSRCR may have some artifacts that appear at the boundaries with large luminance change between the bright and dark regions, which is associated with the convolution and called "halo effect."

Luma-dependent nonlinear enhancement (LDNE) is a luminance based multiscale retinex algorithm.<sup>20</sup> Unlike MSRCR, the LDNE processes only the luminance information of color images instead of all the three spectral bands, significantly reducing the processing time. The color noise

in the shadow/dark areas is suppressed by adding the convolution results instead of multiplying them. LDNE uses a linear process to convert intensity images back to color images, which produces the color rendition more natural than MSRCR and the color adjustment is more controllable and predictable.

Histogram equalization (HE) is a well-established technique for image enhancement. However, HE works well only for scenes that have unimodal or weakly bimodal histograms (i.e., very dark or very bright scenes). For scenes with strongly bimodal histograms (i.e., scenes that contain both very dark and very bright regions), HE performs poorly. Therefore, adaptive histogram equalization (AHE) was introduced.<sup>21</sup> AHE, also called localized or windowed HE, produces a local contrast enhancement by performing HE within a window whose size is adjustable for optimized result. AHE definitely performs better than normal HE. However, the contrast enhancement is so strong that two major problems arise: intensive noise enhancement in "flat" regions and "ring" artifacts at strong edges.<sup>22</sup> To deal with those problems, a generalized version of AHE, contrast-limiting AHE (CLAHE) was designed.<sup>23</sup> CLAHE has more flexibility in controlling the local contrast enhancement by selecting the clipping level of the histogram. Undesired noise amplification is reduced. In addition, the boundary artifacts can also be reduced by using background subtraction.<sup>24</sup> Multiscale AHE (MAHE) is the most advanced variation of HE. Unlike traditional single scale techniques, wavelet-based MAHE is capable of modifying/enhancing image components adaptively based on their spatial-frequency properties.<sup>25</sup> Those advanced HE variations generally have very strong contrast enhancement, which is especially useful in feature extraction applications such as medical imaging for diagnosis. They are not commonly used in processing color images probably because their strong contrast enhancement may lead to excessive noise or artifacts and cause the image to look unnatural.

In the field of computer graphics,<sup>26–31</sup> various algorithms have been developed to deal with a similar problem: how to display a high dynamic range image on a display device with limited dynamic range. However, the techniques developed in both areas may not be shared due to the following two reasons. First, in image processing, the input is an image that has been degraded and recorded by an imaging device of limited dynamic range. In computer graphics, the input is an undistorted array of simulated real-world luminance with high dynamic range. Second, in image processing, the task is to enhance the visibility of imperfect images by compressing the dynamic range and improving the contrast. The subjective correspondence with the original view of the scene generally cannot be maintained. In computer graphics, however, the subjective correspondence must be maintained. Visibility and contrast are simulated to produce visually accurate, not enhanced (changed) images.

Larson *et al.*<sup>26</sup> developed a tone reproduction operator that preserves visibility of high-dynamic-range scenes using a new histogram adjustment technique, based on the population of local adaptation of luminance in a scene. To match subjective viewing experience, the method incorporates models for human contrast sensitivity, glare, spatial acuity, and color sensitivity. This technique and other simi-

lar techniques, developed for computer graphics applications, is not suitable for image enhancement due to its global processing approach and lack of contrast enhancement, which may lead to feature loss or degradation at some areas in the image. Chiu *et al.*<sup>27</sup> were the first in computer graphics to consider that tone mapping should be spatially non-uniform, in other words, the tone mapping should be neighborhood dependent. This method and MSRCR are similar in spirit. Therefore, they share the same problem of halo artifacts. Schlick<sup>28</sup> proposed a simple and rapid nonuniform tone mapping scheme that is dependent on the intensity of each pixel itself. Obviously, it is not adaptive enough to account well for contrast enhancement in image processing.

To eliminate the notorious halo effect, Tumblin and Turk<sup>29</sup> introduced the low-curvature image simplifier (LCIS) hierarchical decomposition of an image. Each stage in this hierarchy is computed by solving partial differential equations inspired by anisotropic diffusion. At each hierarchical level, the method segments the image into smooth (low-curvature) regions, while stopping at sharp discontinuities. The hierarchy describes progressively smoother components of the image intensity (luminance). A set of image details are obtained by subtractions between images at adjacent levels. Tumblin and Turk attenuate the smooth components and reassemble the images to create a low-contrast version of the original while compensating for the wide changes in the illumination field. This method drastically reduces the dynamic range, but tends to overemphasize fine details. The algorithm is computationally intensive and requires the selection of at least eight different parameters. Pattanaik *et al.*<sup>30</sup> presented a tone mapping algorithm, which is made more realistic by incorporating human visual perception behavior into the model. They performed the image decomposition by the Laplacian pyramid (difference-of-Gaussian pyramid) approach. This technique produces dynamic range compressed images with good tonality and accurate color rendering. However, the halo effect in the images produced by their algorithm is much more severe than that produced by MSRCR.

### 3 AINDANE Algorithm

The AINDANE algorithm for the enhancement of color images consists of two major constituents, namely, adaptive luminance enhancement and adaptive contrast enhancement, which are followed by color restoration.

#### 3.1 Adaptive Luminance Enhancement

First, color images in the *RGB* color space are converted to intensity (gray-scale) images using the method defined as

$$I(x,y) = \frac{76.245I_R(x,y) + 149.685I_G(x,y) + 29.07I_B(x,y)}{255} \quad (1)$$

where  $I_R(x,y)$ ,  $I_G(x,y)$ , and  $I_B(x,y)$  represent the *R*, *G*, and *B* values (8-bit), respectively, for the pixel at location  $(x,y)$ . This method is the commonly used NTSC standard for obtaining the luminance (intensity) information of color images on additive color device. Image intensity  $I(x,y)$  is then normalized as

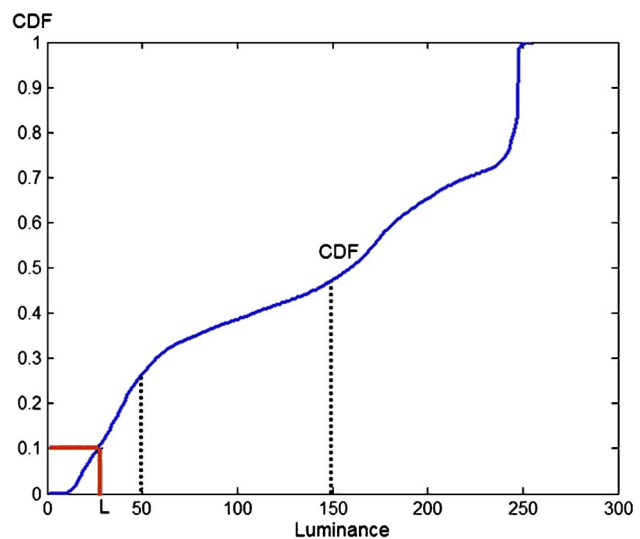


Fig. 1 CDF of an intensity image.

$$I_n(x,y) = \frac{I(x,y)}{255}. \quad (2)$$

Intensity images are treated by an enhancement process to elevate the intensity values of low-intensity (dark) pixels using a specifically designed nonlinear transfer function defined by

$$I'_n = \frac{I_n^{(0.75z+0.25)} + (1 - I_n)0.4(1 - z) + I_n^{(2-z)}}{2}. \quad (3)$$

This process also serves as dynamic range compression. We can observe from Eq. (3) that the nonlinear transfer function is image dependent with a parameter  $z$ , which is related to the image histogram and is defined as

$$z = \begin{cases} 0 & \text{for } L \leq 50 \\ \frac{L-50}{100} & \text{for } 50 < L \leq 150 \\ 1 & \text{for } L > 150, \end{cases}$$

where  $L$  is the intensity level corresponding to a cumulative distribution function (CDF) of 0.1. That is, when more than 90% of all pixels have intensity higher than 150,  $z$  is 1. If 10% or more of all pixels have intensity lower than 50,  $z$  is 0. For all other cases, when the gray scale of 10% or more of all pixels is higher than 50 and lower than 150,  $z = (L-50)/100$ . Obviously,  $L$  is used as an indication to determine how dark the 10% of pixels in an image are. If they are really dark (e.g.,  $L < 50$ ), luminance must be enhanced more. If they are not that dark (e.g.,  $L \approx 100$ ), less luminance enhancement will be required. If most of the pixels have sufficient brightness (e.g.,  $L > 150$ ), no luminance enhancement will be needed. Figure 1 illustrates the CDF of an intensity image with respect to the gray-level  $L$ . The range of  $z$  and the relationship between  $z$  and  $L$  are determined empirically based on image enhancement experiments and authors' judgment. In addition,  $z$  can be a user adjustable parameter for manually tuning the luminance enhancement process.

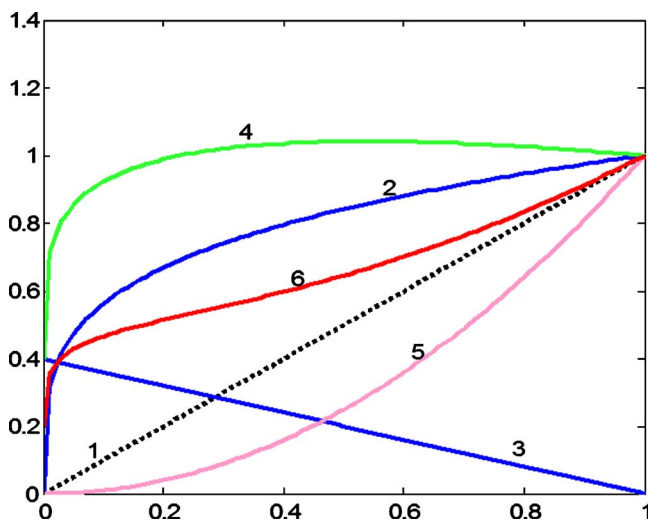


**Fig. 2** Nonlinear transfer function (curve 6: when  $z=0$ ) for luminance enhancement.

The transfer function is actually a combination of three simple mathematical functions and it is graphically shown as the curve 6 ( $z=0$ ) in Fig. 2 with a dotted straight line (line 1) for comparison, which in fact represents the identity transformation. The first two terms in Eq. (3) are plotted as curve 2 and line 3, respectively, and the summation of them yields curve 4. The last term in Eq. (3) is shown in the graph as curve 5. The addition of curves 4 and 5 after normalization [division by 2 in Eq. (3)] produces the transfer function shown as curve 6. It can be seen that this transformation largely increases the luminance of darker pixels (regions) while brighter pixels (regions) are less enhanced. Therefore, the line shape of the transfer function is important no matter what mathematical functions are used. Simple functions are applied for faster computation. Similar curve shapes produced by other types of functions will have similar effects on luminance enhancement if they are used as the transfer function. Note that this transfer function is designed for the purpose of luminance enhancement and it can also provide appropriate dynamic range compression from which good enhanced results will be obtained through the contrast enhancement process. The effect of  $z$  on the transfer function is illustrated in Fig. 3. As  $z$  approaches 1, the transfer function curve gets closer to the identity transformation. The graph indicates that brighter images (with larger  $z$ ) have less luminance enhancement to prevent overenhancement.

### 3.2 Adaptive Contrast Enhancement

After luminance enhancement, the contrast enhancement process is applied to restore the contrast of the luminance-enhanced images, which has been degraded during the previous process (the images look grayed out). The restored contrast may be even higher than that of original images for high visual quality. However, the normal global contrast enhancement technique is unable to fulfill that request. It simply increases the luminance for bright pixels and decreases the luminance for the dark pixels. As a result, the dynamic range can be significantly expanded. On the other hand, this method has limited performance for bringing out

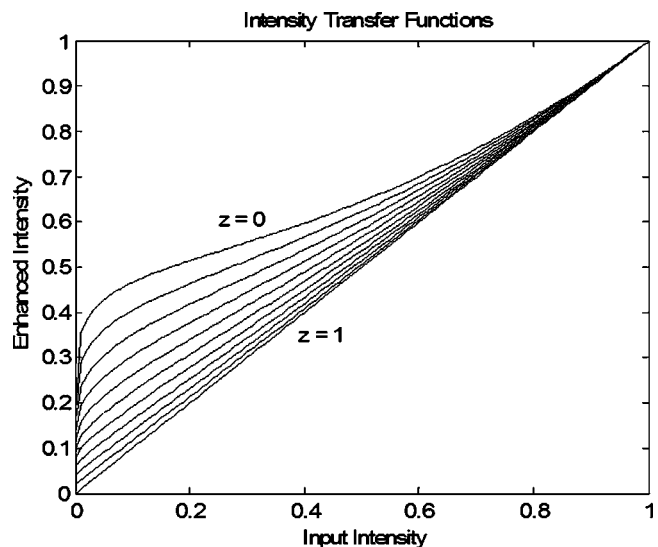


**Fig. 3** Nonlinear transfer functions with different  $z$  values ( $z=0$ , top curve;  $z=1$ , bottom line).

fine details where adjacent pixels have small luminance differences because the surrounding pixels are not considered when one pixel is being processed. Therefore, a surrounding pixel (neighborhood)-dependent contrast enhancement technique must be implemented to achieve sufficient contrast for image enhancement without losing the dynamic range compression. While an image is processed with such a method, pixels with the same luminance can have different outputs depending on their neighboring pixels. When surrounded by darker or brighter pixels, the luminance of the pixel being processed (the center pixel) will be boosted or lowered, respectively. In this way, picture contrast and fine details can be sufficiently enhanced while dynamic range expansion can be controlled without degrading image quality.

The luminance information of surrounding pixels is obtained by using 2-D discrete spatial convolution with a Gaussian kernel, which in essence is one type of neighborhood averaging. A Gaussian kernel is used due to its closeness to the way in which human visual system works. The standard deviation (also called scale) of the 2-D Gaussian distribution determines the size of the neighborhood. The 2-D Gaussian function  $G(x,y)$  is obtained as

$$G(x,y) = K \exp\left[-\frac{(x^2 + y^2)}{c^2}\right], \quad (4)$$

where  $K$  is determined by

$$\int \int K \exp\left[-\frac{(x^2 + y^2)}{c^2}\right] dx dy = 1, \quad (5)$$

and  $c$  is the scale or Gaussian surround space constant. The 2-D discrete convolution is carried out on the original intensity image  $I(x,y)$  of size  $M \times N$  as

$$I_{\text{conv}}(x,y) = \sum_{m=0}^{M-1} \sum_{n=0}^{N-1} I(m,n) G(m+x, n+y), \quad (6)$$

which is computed by multiplication in frequency domain. After the surrounding intensity information is obtained by 2-D convolution, the center pixel's intensity is compared with the convolution result. These two operations are both carried out on the original image. If the center pixel's intensity is higher than the average intensity of surrounding pixels, the corresponding pixel on the luminance-enhanced image will be pulled up, otherwise it will be pulled down. As a result, the contrast of the luminance-enhanced image can be adaptively improved without counteracting the effect of luminance enhancement. The center-surround contrast enhancement is carried out as defined in the following two equations:

$$S(x,y) = 255 I'_n(x,y)^{E(x,y)}, \quad (7)$$

where the exponent is defined by

$$E(x,y) = r(x,y)^P = \left[ \frac{I_{\text{conv}}(x,y)}{I(x,y)} \right]^P, \quad (8)$$

$S(x,y)$  is the pixel intensity after contrast enhancement, and  $r(x,y)$  is the intensity ratio between  $I_{\text{conv}}(x,y)$  and  $I(x,y)$ ;  $P$  is an image dependent parameter, which is used to tune the contrast enhancement process. If the contrast of original image is poor,  $P$  will be larger and further increase the contrast enhancement. Also,  $P$  is determined by the global standard deviation  $\sigma$  of the input intensity image  $I(x,y)$  as

$$P = \begin{cases} 3 & \text{for } \sigma \leq 3 \\ \frac{27 - 2\sigma}{7} & \text{for } 3 < \sigma < 10 \\ 1 & \text{for } \sigma \geq 10. \end{cases}$$

According to this definition,  $P$  is 1 if  $\sigma$  is greater than or equal to 10, and  $P$  equals to 3 when  $\sigma$  is less than or equal to 3. For all other cases, there is a linear relationship between the power  $P$  and  $\sigma$ . This relationship is determined based on image enhancement experiments. Here, the global standard deviation  $\sigma$  of  $I(x,y)$  is considered as an indication of the contrast level of the original intensity image. Note that  $P$  can be changed by users to manually adjust the contrast enhancement process.

The contrast enhancement process defined in Eqs. (7) and (8) is actually an intensity transformation process and can be understood using Fig. 4. Since  $I'_n$  is normalized to 1,  $I'_n(x,y)^{E(x,y)}$  will be larger than  $I'_n(x,y)$  if  $E(x,y)$  is less than 1 [i.e., the center pixel is brighter than surrounding pixels leading to  $r(x,y) < 1$ ]. Otherwise, if  $E(x,y)$  is larger than 1 [i.e., the center pixel is darker than the surrounding pixels with  $r(x,y) > 1$ ],  $I'_n(x,y)^{E(x,y)}$  will be smaller than  $I'_n(x,y)$ . In this way, the contrast of the luminance-enhanced image can be improved. Here, the ratio  $r(x,y)$  is obtained from the original intensity image  $I(x,y)$  and its lowpass filtered result  $I'(x,y)$ , since the contrast information in the luminance enhanced image has been changed and degraded during the nonlinear luminance enhancement process.

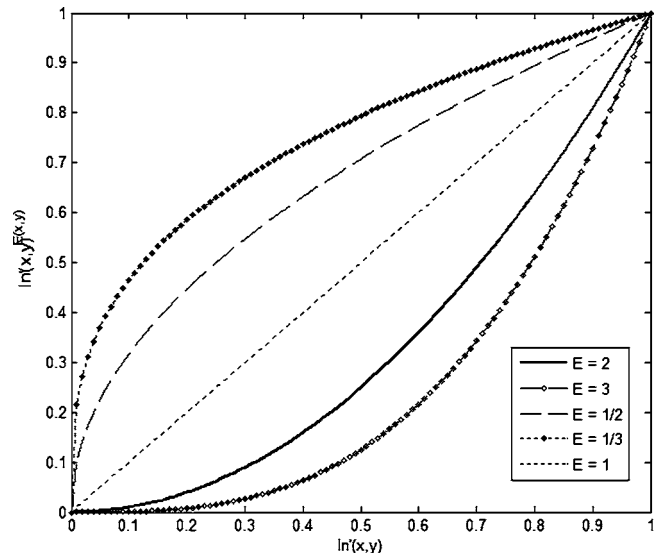


Fig. 4 Intensity transformation for contrast enhancement.

For better results of image enhancement, contrast enhancement is performed with multiple convolution results using different scales. The final output is a linear combination of the contrast enhancement results based on multiple scales. A convolution with a small scale, such as a few neighboring pixels, can provide luminance information about the nearest neighborhood pixels, while the convolution with a large scale comparable to the image dimensions can provide the information about the large-scale luminance variation over the whole image. Generally, contrast enhancement with smaller scale convolutions tend to enhance local contrast or fine details, and the contrast enhancement with larger scale convolutions can produce a global tonality closing to the original image for smooth and natural looking results. A medium scale can provide a mixture of both details and image rendition. Obviously, convolutions with multiple scales can yield more complete information on the image's luminance distribution, and hence lead to more balanced image enhancement. However, if faster processing or certain special effect is wanted, a single-scale convolution can be used for contrast enhancement. For example, only a medium scale convolution can be applied to achieve fast processing while the result is still acceptable. The contrast enhancement with multiscale convolutions can be described by the following equations:

$$G_i(x,y) = K \exp \left[ \frac{-(x^2 + y^2)}{c_i^2} \right], \quad (9)$$

$$I_{\text{conv},i}(x,y) = \sum_{m=0}^{M-1} \sum_{n=0}^{N-1} I(m,n) G_i(m+x, n+y), \quad (10)$$

$$E_i(x,y) = r_i(x,y)^P = \left[ \frac{I_{\text{conv},i}(x,y)}{I(x,y)} \right]^P, \quad (11)$$

$$S_i(x,y) = 255[I'_n(x,y)^{E_i(x,y)}], \quad (12)$$

$$S(x,y) = \sum_i w_i S_i(x,y), \quad (13)$$

where  $c_i$  ( $i=1,2,3,\dots$ ) represents different scales, and  $w_i$  is the weight factor for each contrast enhancement output  $S_i(x,y)$ . By default,  $w_i=1/n$ ,  $i=1,2,3,\dots,n$  ( $n$  is the number of scales), based on our image enhancement experiments. Note  $n=3$  is typical and yields enhanced images having a well-balanced and natural visual effect. Both fine details and overall tonality can be accounted for in the output images. In this work, the three scales, 5, 20, and 120, are commonly used, or a simple guide can be followed: the smallest scale is 1 to 5% of the image size, the medium and the largest scales are 10 to 15 and 25 to 45% of the image size, respectively. Usually  $c_i$ ,  $w_i$ , and  $n$  are fixed in our image enhancement experiments, while they can still be changed to obtain optimal result or certain special effect.

### 3.3 Color Restoration

So far, both luminance and contrast enhancements have been performed in the luminance space. The enhanced color image can be obtained through a linear color restoration process based on the chromatic information contained in the input image. Mathematically, the color restoration process for images in *RGB* color space can be expressed as:

$$S_j(x,y) = S(x,y) \frac{I_j(x,y)}{I(x,y)} \lambda_j, \quad (14)$$

where  $j=r,g,b$  represents the *R*, *G*, *B* spectral band, respectively, and  $S_r$ ,  $S_g$ , and  $S_b$  are the RGB values of the enhanced color image. A parameter  $\lambda$  is introduced here to manually adjust the color hue of the enhanced color images, and  $\lambda$  is a constant smaller than but very close to 1, which takes different values in different spectral bands. When all  $\lambda$ s are equal to 1, Eq. (14) can preserve the chromatic information of the input color image for minimal color shifts.

## 4 Experimental Results and Discussion

The proposed algorithm was applied to enhance a large number of digital images for performance evaluation and comparison with other algorithms. Some typical results as well as detailed discussion about various characteristics of the algorithm are presented in this section.

Images enhanced with various parameter values are illustrated in Fig. 5. The effects of those parameters are clearly shown and are in agreement with the description provided in the previous section. If the parameters are manually adjusted, image quality can be changed to obtain optimized result. With the self-adaptiveness implemented in our algorithm, the parameter adjustment can be conducted automatically according to the quality of the original image. Automatic tuning can produce results better than or at least equivalent to those obtained with default parameter values.

The AINDANE algorithm was applied to process a large number of digital images taken by digital cameras under varying lighting conditions. The enhanced images have good quality, with fine details, well-balanced contrast and luminance across the whole image, and natural color rendition of appropriate color saturation. AINDANE has various

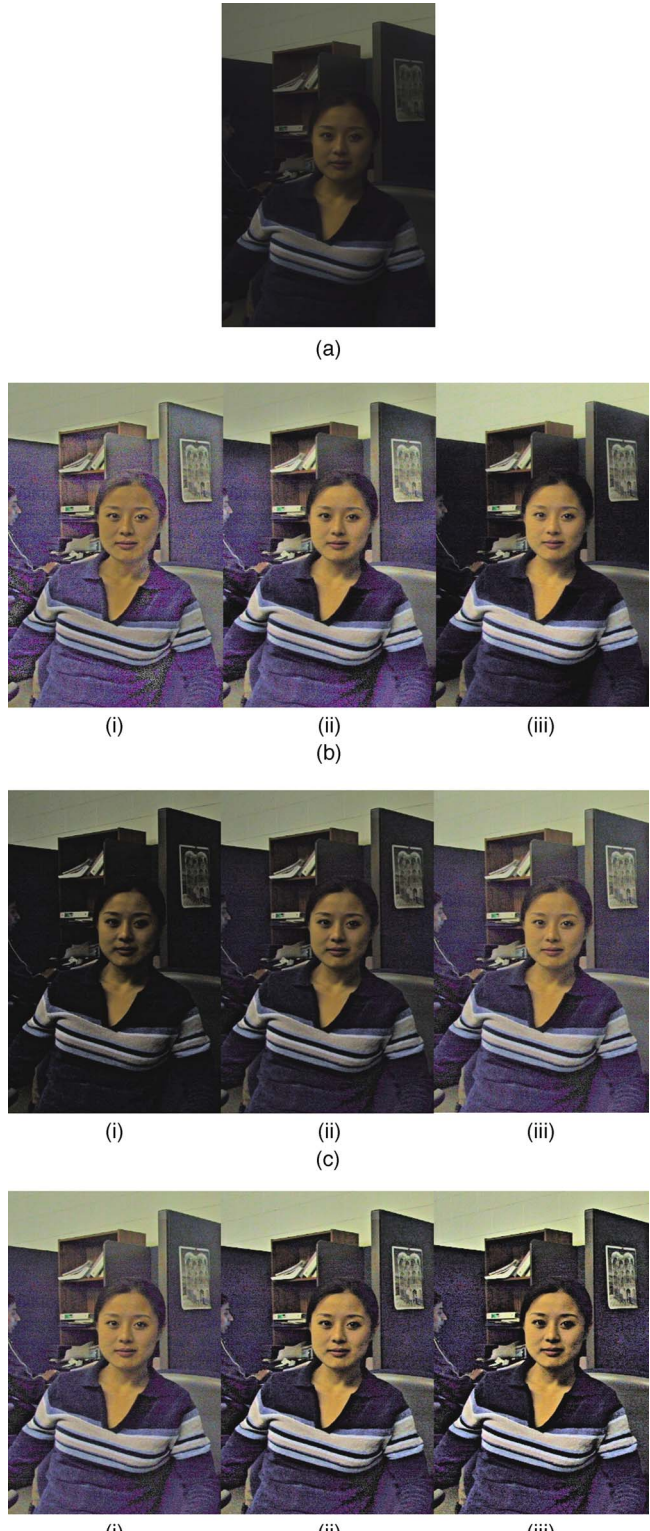


**Fig. 5** Image enhancement results with various parameter values: (a) original image; (b) images enhanced using single scale convolution and with  $z=0$  and  $P=1$ : (i)  $c=5$ , (ii)  $c=20$ , and (iii)  $c=240$ ; (c) images enhanced by multiscale  $c$  and with different  $z$  values and  $P=1$ : (i)  $z=1$ , (ii)  $z=0.5$ , and (iii)  $z=0$ ; and (d) images enhanced by multiscale  $c$  and with different  $P$  values and  $z=0$ : (i)  $P=1$ , (ii)  $P=2$ , and (iii)  $P=3$ .



(a)



(b)



(c)

**Fig. 6** Luminance enhancement with adaptive factor  $z$  of different values: (a) original image, (b) result obtained from INDANE ( $z=0$ ), and (c) result obtained from AINDANE ( $z \neq 0$ ).

adjustable parameters, which have been finely tuned by conducting several experiments to achieve consistently high quality results for different types of images. Some of the parameters are image dependent and are introduced to make the algorithm more adaptive. For example, the parameter  $z$  in Eq. (3) (nonlinear transfer function) is determined by the image's histogram and is used to adjust the luminance enhancement to avoid over or insufficient enhancement of luminance. The example in Fig. 6 shows the effect of  $z$  on enhanced images. The original image was taken with sufficient illumination. The enhanced image



(a)



(b)



(c)

**Fig. 7** Contrast enhancement with adaptive factor  $P$  of different values: (a) original image, (b) result obtained by INDANE ( $P=1$ ), and (c) result obtained by AINDANE ( $(P \neq 1)$ ).

processed<sup>32</sup> by INDANE (without adaptiveness,  $z=0$  and  $P=1$ ) looks worse than the original in terms of contrast and color saturation. However, AINDANE ( $z \neq 0$ ) produced a better result in which the person's face looks more real with outlines and edges being clearly brought out. The general contrast is improved by AINDANE.

Parameter  $P$  is another image-dependent parameter used for contrast enhancement in AINDANE. It is used to ensure that the contrast of low-contrast images will be increased to obtain good visual effect. The example illustrated in Fig. 7 shows the effect of  $P$  on image enhancement. The original image was captured with insufficient illumination under the caps and has poor contrast on the wood board. AINDANE with adaptive control parameter ( $P \neq 1$ ) produces an enhanced image with much higher contrast than that obtained

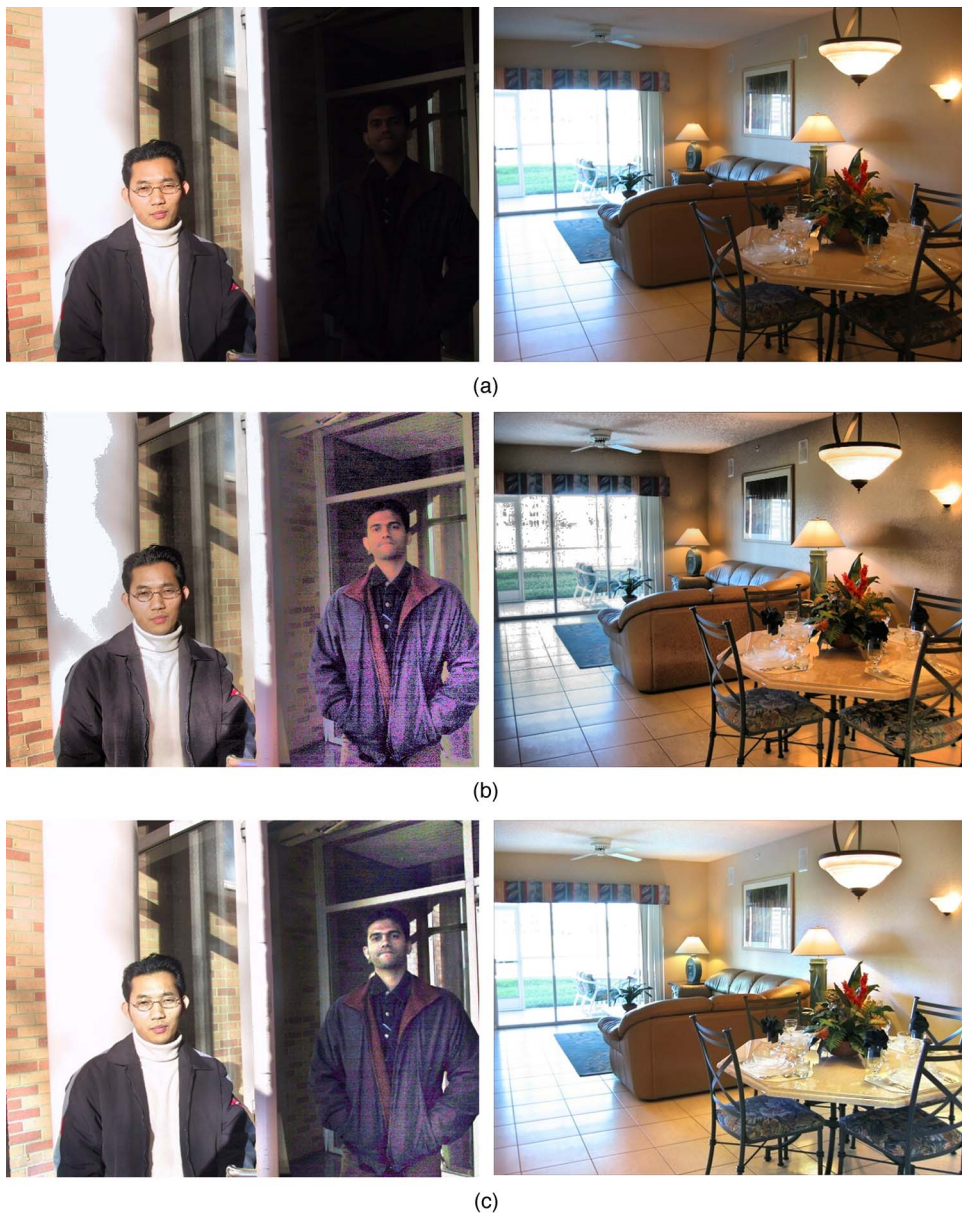


**Fig. 8** Image enhancement comparison: (a) original images, (b) AHE, (c) retinex, (d) MSRCR, (e) INDANE, and (f) AINDANE using two sample images captured under non-uniform lighting environment.

by INDANE that has no adaptive-ness ( $P=1$ ). Grains in the wood region became obvious and maintain the overall luminance level.

It can be found that AINDANE shares certain similarity with MSRCR and LDNE. However, AINDANE has several advantages over MSRCR and LDNE in terms of color rendition and flexibility in algorithm tuning. In MSRCR, each spectral band is individually processed, and color restoration for improving color constancy is realized using a non-linear process. These processes might produce some color artifacts, which cannot be predicted from the original image, making enhanced images look unnatural or incorrect in colors. As in MSRCR, dynamic range compression and contrast enhancement are implemented jointly in LDNE,

which makes the algorithm tuning more difficult than AINDANE where the two processes are separated and can be tuned independently.

In all of the three enhancement techniques, the convolution result is compared with the center pixel in the form of the intensity ratio. However, AINDANE is completely different from MSRCR and LDNE in the way it uses this ratio. AINDANE performs a power-law transformation to the luminance-enhanced image using the ratio as the exponent. As a result, the image's contrast can be enhanced. MSRCR and LDNE, however, perform a logarithmic transformation to the ratio followed by a gain-offset process, and both dynamic range compression and contrast enhancement are accomplished at the same time.

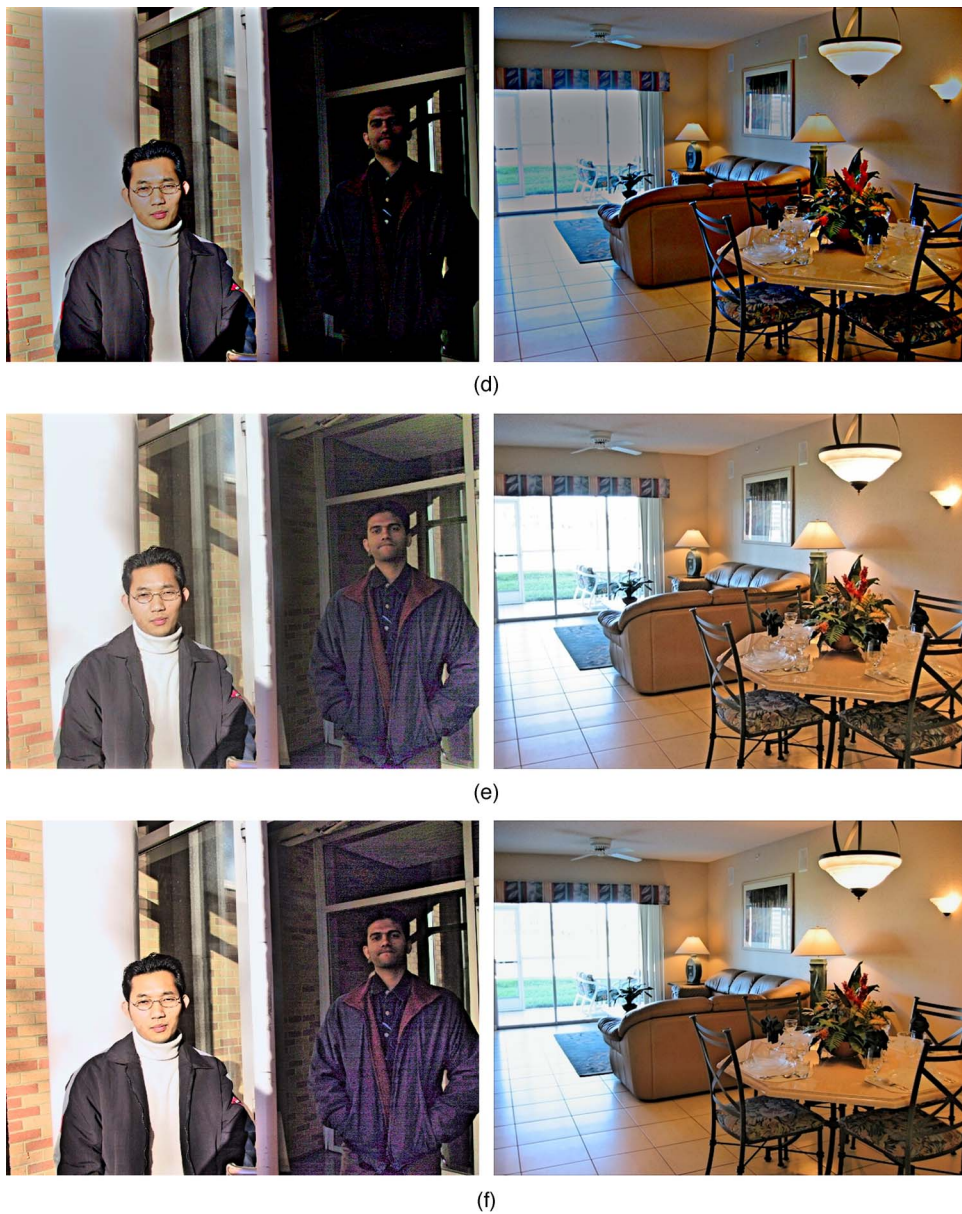


**Fig. 8 (Continued).**

In Fig. 8, two sample images are provided for comparison among the performance of retinex, MSRCR, INDANE, AINDANE and AHE. Retinex is realized using the Matlab® code provided in Ref. 2 by Frankle and McCann. A commercial software PhotoFlair® ([www.truview.com](http://www.truview.com)) is used to implement MSRCR. It can be observed that the images processed by AINDANE have a higher visual quality than those processed by MSRCR, AHE, and INDANE. AINDANE yields higher color accuracy and a better balance between the luminance and contrast across the whole image due to its adaptiveness and flexibility involved in the processing. In the first sample image, AHE brings out the person standing in the shadow. However, artifacts appear on the white pillar and the face of the person in sunshine gets even dimmer. The whole image looks quite unnatural with such a brightness distribution. In the second sample image, AHE produces a lot of artifacts and

noise and luminance enhancement is not sufficient. The images enhanced by retinex demonstrate high contrast and good illuminance. However, its color constancy seems not to be working well at some places (the face of the man in shadow is much whiter than it should be, and the color of different parts of the table top is inconsistent) and the lightness rendition looks a little unnatural (the table top is too bright). In addition, both MSRCR and retinex show much more visible halo effect than our proposed algorithm. It is also found that MSRCR seems to have some difficulty enhancing images in nonuniform lighting conditions. The luminance enhancement in the darker regions is insufficient. It is even worse in the sense that the brightness of some of the highlighted areas is incorrectly reduced to yield a tonality difference from the original. More comparisons between MSRCR, retinex, and AINDANE are provided in Fig. 9. The previously discussed issues, incorrect lightness and

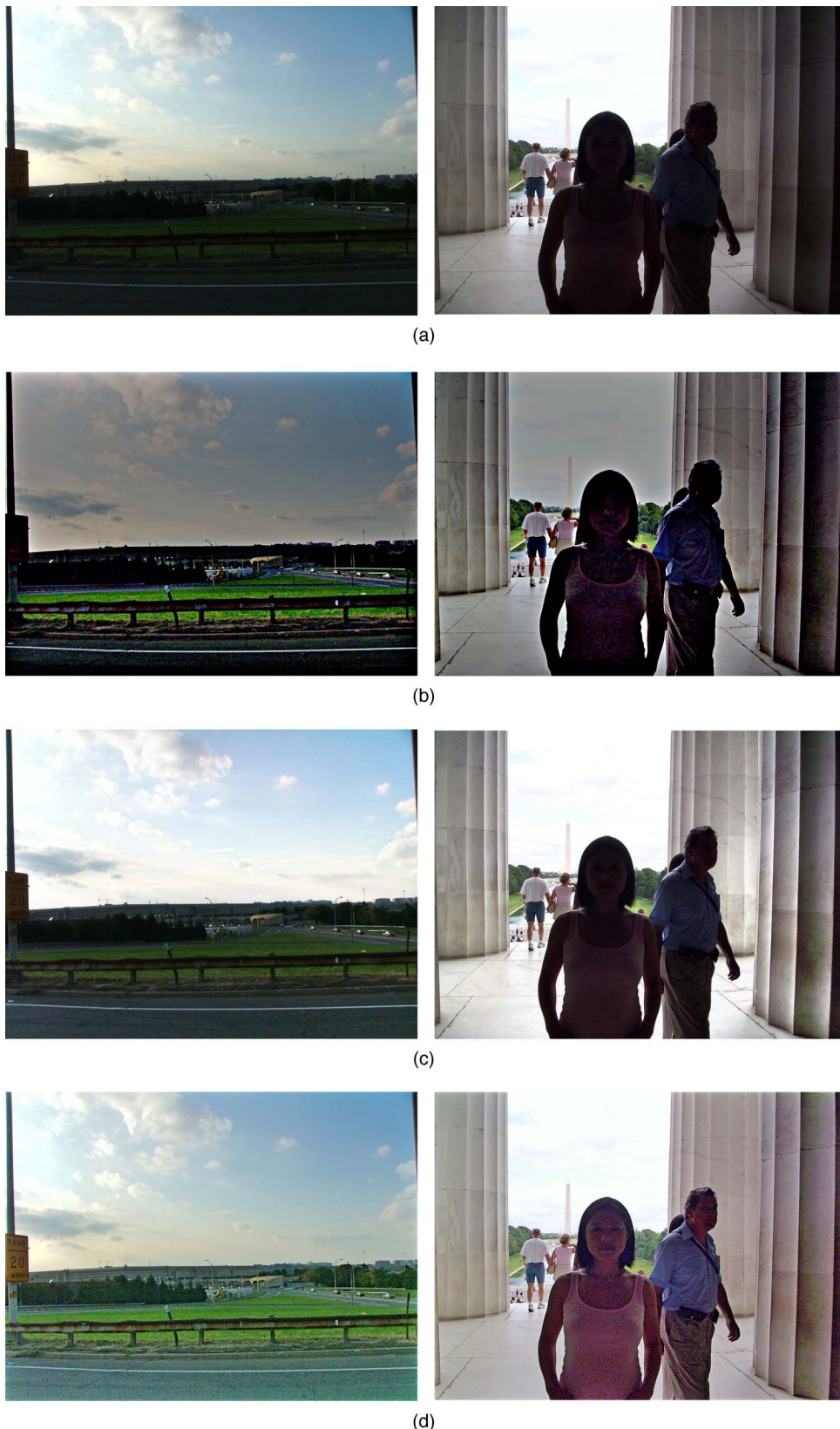


**Fig. 9** Comparison among MSRCR, retinex, and AINDANE: (a) original images and images (b) enhanced results by MSRCR, (c) enhanced results by retinex, and (d) enhanced results by AINDANE.

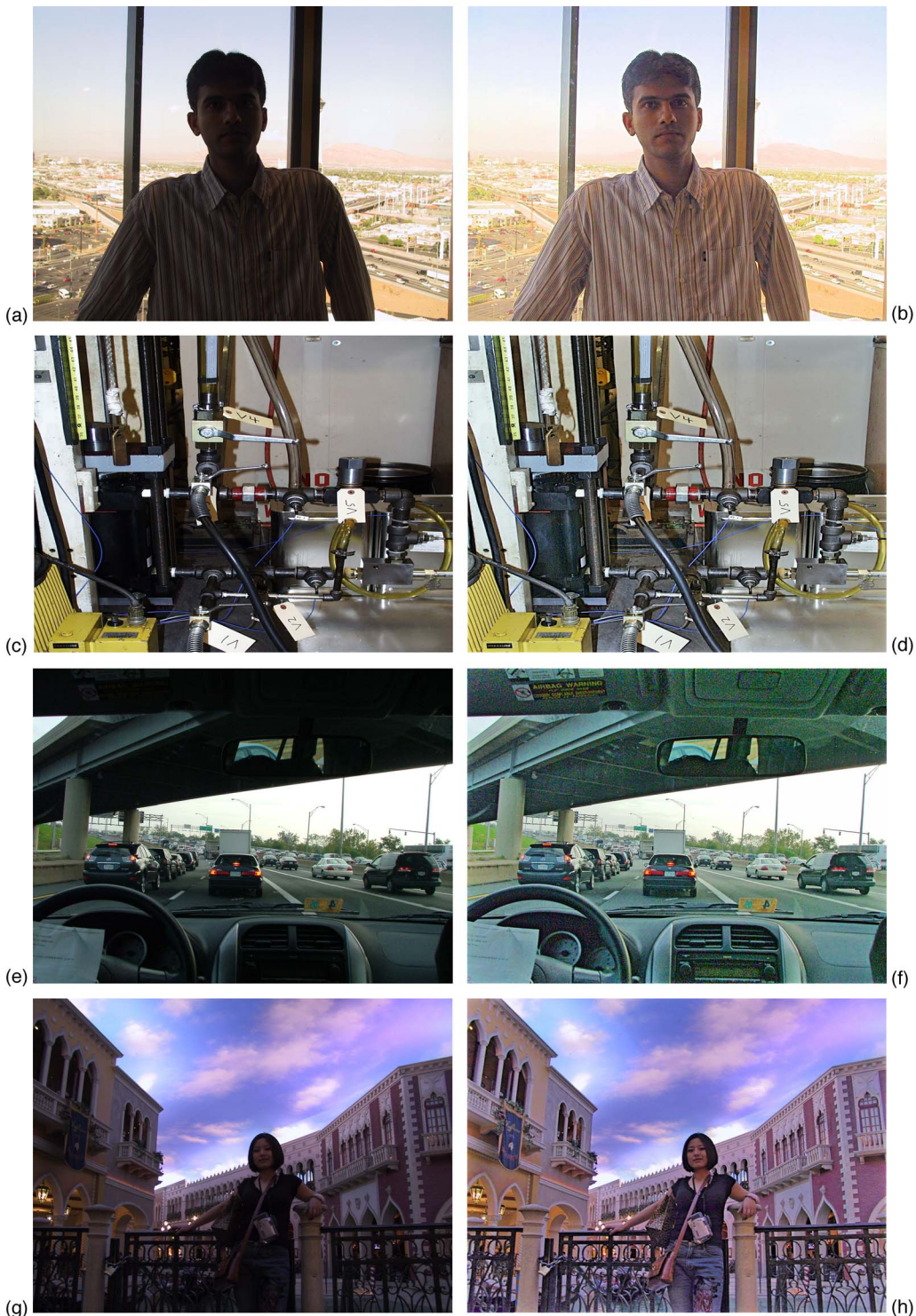


**Fig. 10** Image enhancement results obtained by AINDANE. Left column: original images; right column: enhanced images.

color rendition, as well as insufficient luminance enhancement, are still clearly visible. Obviously, MSRCR provides strong contrast enhancement but the luminance enhancement is poor. The luminance of high-brightness regions are even largely degraded after enhancement. In addition, the color rendition looks unnatural with high color saturation. Retinex performs much better than MSRCR. However, its

color correction capability may also create incorrect colors. For example, the cloud in the left image is bleached although the cloud color is correct in the original image. Moreover, both MSRCR and retinex provide insufficient luminance enhancement to the woman's face because of the highlighted background and the unbalancing between the luminance enhancement and contrast enhancement. On the

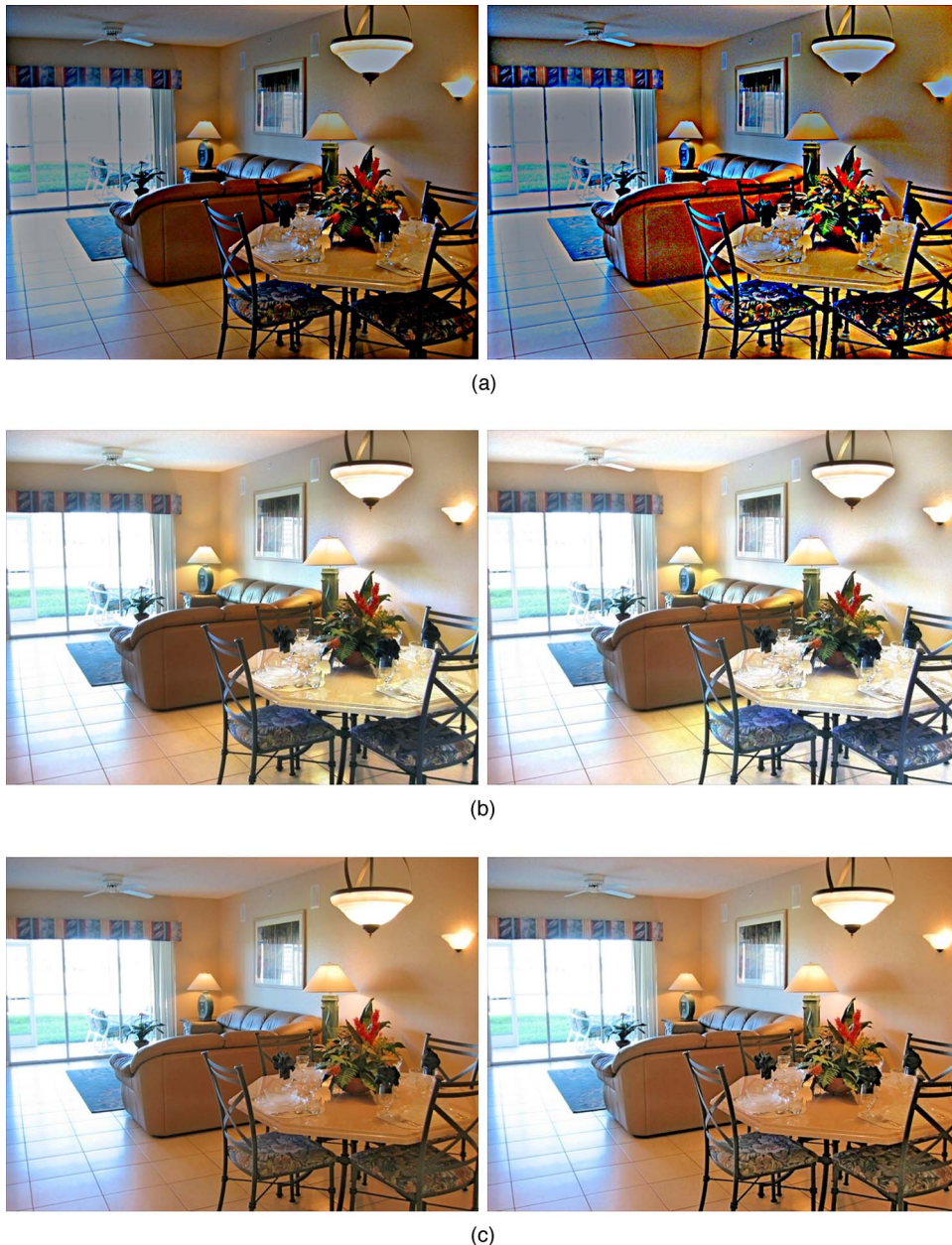


**Fig. 11** Robust evaluation: (a) MSRCR, (b) retinex, and (c) AINDANE. Left column: enhanced results from the original images (enhanced once); right column: enhanced results from the left column images (enhanced twice).

other hand, the proposed algorithm generally performs well on those test images showing a more balanced result between luminance enhancement and contrast enhancement and no incorrect colors created.

Some more example images enhanced by AINDANE are shown in Fig. 10. These images were captured by Canon digital camera under various illumination conditions. The visual quality of these images is significantly improved after image enhancement. Shadows or dark images are brightened and are made more visible by bringing out more details, features, and colors. The enhanced images look natural with enhanced feature visibility, accurate color rendition, and good balance between brightness and contrast.

To test the robustness of AINDANE, the algorithm was

applied to images twice: the first enhancement processing was carried out on the original image, then the second enhancement processing was performed on the output image from the first enhancement. One example of the results [the original image shown in Fig. 8(a) right side] is presented in Fig. 11, accompanied by the results produced by MSRCR and retinex. Obviously, AINDANE produces the minimal change after the second enhancement while many problems arise in images produced by MSRCR and retinex. Incorrect lightness and color rendition, halo effect, and image noise become much more visible after the second enhancement. It is believed that the higher robustness of AINDANE is due to the modest contrast enhancement and self-adaptiveness.

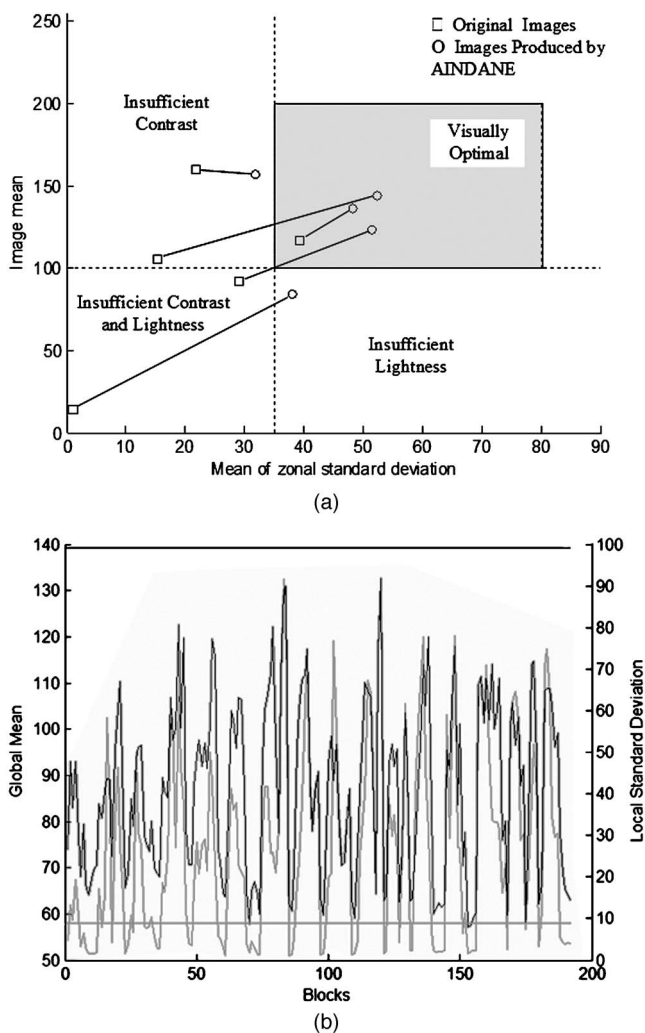


**Fig. 12** Statistical characteristics of images before and after image enhancement: (a), image mean (global mean) versus mean of zonal standard deviation and (b), global mean and local standard deviation at each block (gray straight line and gray curve: global mean and local standard deviation of the original image, dark straight line and dark curve: global mean and local standard deviation of the enhanced image).

The enhanced images obtained by AINDANE were also evaluated by using the statistical method proposed by Jobson *et al.*<sup>33</sup> The statistical properties of images, image mean, and the mean of zonal standard deviation, are used to assess the visual quality of images in terms of lightness and contrast, which are directly associated with those statistical parameters. The overall lightness is measured by the image mean while the overall contrast is evaluated by taking the mean of the regional standard deviations. As shown in Fig. 12(a), based on the statistical properties, the image quality can be classified into four types (four regions in the graph defined by the two dashed lines and the coordinate axes): insufficient contrast and lightness, insufficient lightness, insufficient contrast, and visually optimal (sufficient contrast and lightness). The data points of several original images and the corresponding enhanced images are plotted in squares and circles respectively in the figure, which are connected via a straight line, indicating the direction of the change in image enhancement. The effect of image enhancement

**Table 1** Comparison of AINDANE and MSRCR in processing time

Image Size (pixels)	Processing Time by AINDANE (s)	Processing Time by MSRCR (s)
360 × 240	0.25	1.2
640 × 480	1.4	4
1024 × 768	2.8	8
2000 × 1312	6.7	18

is clearly depicted by transferring images into visually optimal region. Based on the results of our image enhancement experiments, most of the enhanced images are located inside the visually optimal region, except those images obtained under extremely low illumination. For one specific test image ("Living room"), we also plotted the global means and local standard deviations of all blocks (block size:  $40 \times 40$ ) of the image before and after image enhancement [shown in Fig. 12(b)]. We can see that the global luminance and local contrast enhancement is dramatic.

## 5 Computational Speed

The processing time required for enhancing images of different sizes is compared between AINDANE and MSRCR. The computing platform is an Intel Pentium 4 system, which has a CPU running at 3.06 GHz and 1 Gbyte of memory. The operating system is Windows XP® Professional Edition. A commercial digital image processing software, PhotoFlair® version 2.0 (TruView Imaging Company), was used to process images using MSRCR algorithm, while a Windows version of AINDANE implemented in C++ applied to process the same set of images. The processing time required to enhance images of various sizes is provided in Table 1 for comparison between AINDANE and MSRCR. Generally, the processing time of AIDANE is approximately 30% of that of MSRCR. This is because fast Fourier transform (FFT) computations occupy most of the processing time, and only the intensity image (equivalent to one color band) is processed with an FFT in AINDANE to obtain neighborhood averaging while all three color bands are processed separately with an FFT in MSRCR. Therefore, AINDANE is more suitable for rapid applications.

## 6 Conclusion

A new nonlinear image enhancement algorithm AINDANE was developed to improve the visual quality of digital images captured under insufficient or nonuniform lighting conditions. The image enhancement algorithm is composed of two separate processes: the adaptive luminance enhancement (dynamic range compression) and the adaptive contrast enhancement. The combination of the two processes is believed to make the algorithm more flexible and easier to control. The adaptiveness of the algorithm, depending on the statistical information of the input images, was realized in AINDANE to automatically refine the image quality. AINDANE was tested with a large number of images. The enhanced images processed by AINDANE have improved

visual quality compared with those produced by MSRCR and other techniques in terms of a better balance between luminance and contrast. Colors are better preserved compared to MSRCR. Moreover, the processing speed of AINDANE is much faster than that of MSRCR. Based on the enhancement results, AINDANE algorithm would be a promising image enhancement technique that can be useful in many applications.

## References

1. H. Kolb, "How the retina works," *American Scientist* **91**(1) (2003).
2. B. Funt, F. Ciurea, and J. McCann, "Retinex in matlab," in *Proc. CIC'8 8th Color Imaging Conf.* pp. 112–121, Imaging Science & Technology Society, Scottsdale, AZ (2000).
3. D. J. Jobson, Z. Rahman, and G. A. Woodell, "Properties and performance of a center/surround retinex," *IEEE Trans. Image Process.* **6**(3), 451–462 (1997).
4. E. Land and J. McCann, "Lightness and retinex theory," *J. Opt. Soc. Am.* **61**(1), 1–11 (1971).
5. E. Land, "Recent advances in retinex theory and some implications for cortical computations," *Proc. Natl. Acad. Sci. U.S.A.* **80**, 5163–5169 (1983).
6. E. Land, "Recent advances in retinex theory," *Vision Res.* **26**(1), 7–21 (1986).
7. J. McCann, S. McKee, and T. Taylor, "Quantitative studies in retinex theory, a comparison between theoretical predictions and observer responses to the color Mondrian experiments," *Vision Res.* **16**, 445–458 (1976).
8. J. Franke and J. McCann, "Method and apparatus for lightness imaging," U.S. Patent No. 4,384,336 (May 17, 1983).
9. E. Land, "An alternative technique for the computation of the descriptor in the retinex theory of color vision," *Proc. Natl. Acad. Sci. U.S.A.* **83**, 2078–3080 (1986).
10. J. McCann, "Lessons learned from Mondrians applied to real images and color gamuts," in *Proc. IS&T/SID 7th Color Imaging Conf.*, pp. 1–8 (1999).
11. R. Sobol, "Improving the retinex algorithm for rendering wide dynamic range photographs," in *Proc. SPIE* **4662**, 341–348 (2002).
12. A. Rizzi, C. Gatta, and D. Marini, "From retinex to ACE: Issues in developing a new algorithm for unsupervised color equalization," *J. Electron. Imaging* **13**(1), 75–84 (2004).
13. Z. Rahman, D. Jobson, and G. Woodell, "Multiscale retinex for color image enhancement," *Proc. IEEE Int. Conf. on Image Processing*, IEEE (1996).
14. Z. Rahman, D. Jobson, and G. Woodell, "Multiscale retinex for color rendition and dynamic range compression," in *Applications of Digital Image Processing XIX*, A. G. Tescher, Ed., *Proc. SPIE* **2847**, 183–191 (1996).
15. D. Jobson, Z. Rahman, and G. Woodell, "A multi-scale retinex for bridging the gap between color images and the human observation of scenes," *IEEE Trans. Image Process.* **6**, 965–976 (1997).
16. Z. Rahman, G. Woodell, and D. Jobson, "A comparison of the multiscale retinex with other image enhancement techniques," in *Proc. IS&T 50th Anniversary Conf.*, pp. 426–431, IS&T (1997).
17. T. Watanabe, Y. Kuwahara, A. Kojima, and T. Kuroswa, "Improvement of color quality with modified linear multi-scale retinex," *Proc. SPIE* **5008**, 59–69 (2003).
18. K. Barnard and B. Funt, "Analysis and improvement of multi-scale retinex," in *Proc. IS&T/SID 5th Color Imaging Conf.: Color Science, Systems and Applications*, pp. 221–226, Scottsdale, AZ (1997).
19. K. Barnard, G. Finlayson, and B. Funt, "Color constancy for scenes with varying illumination," in *Proc. 4th Eur. Conf. on Computer Vision*, Vol. II, pp. 1–15 (1996).
20. L. Tao and V. K. Asari, "Modified luminance based MSRCR for fast and efficient image enhancement," in *Proc. IEEE Int. Workshop on Applied Imagery and Pattern Recognition, AIPR-2003*, pp. 174–179, Washington, DC (2003).
21. S. M. Pizer, J. B. Zimmerman, and E. Staab, "Adaptive grey level assignment in CT scan display," *J. Comput. Assist. Tomogr.* **8**, 300–305 (1984).
22. J. B. Zimmerman, S. B. Cousins, K. M. Hartzell, M. E. Frisse, and M. G. Kahn, "A psychophysical comparison of two methods for adaptive histogram equalization," *J. Digit Imaging* **2**, 82–91 (1989).
23. S. M. Pizer and E. P. Amburn, "Adaptive histogram equalization and its variations," *Comput. Vis. Graph. Image Process.* **39**, 355–368 (1987).
24. K. Rehm and W. J. Dallas, "Artifact suppression in digital chest radiographs enhanced with adaptive histogram equalization," *Proc. SPIE* **1092**, 290–300 (1989).
25. Y. Jin, L. M. Fayad, and A. F. Laine, "Contrast enhancement by multiscale adaptive histogram equalization," *Proc. SPIE* **4478**, 206–213 (2001).
26. G. W. Larson, H. Reschmeier, and C. Piatko, "Visibility matching tone reproduction operator for high dynamic range scenes," *IEEE Trans. Vis. Comput. Graph.* **3**(4), 291–306 (1997).
27. K. Chiu, M. Herf, P. Shirley, S. Swamy, C. Wang, and K. Zimmerman, "Spatially non-uniform scaling functions for high contrast images," in *Proc. Graphics Interface*, pp. 182–191 (1993).
28. C. Schlick, "Quantization techniques for visualization of high dynamic range pictures," in *Photorealistic Rendering Techniques, Proc. 5th Eurographics Rendering Workshop*, pp. 7–20 (1994).
29. J. Tumblin and G. Turk, "LCIS: a boundary hierarchy for detail-preserving contrast reduction," in *SIGGRAPH 99 Conf. Proc., Computer Graphics Annu. Conf. Series*, pp. 83–90, ACM (1999).
30. S. N. Pattanaik, J. A. Ferwerda, M. D. Fairchild, and D. P. Greenberg, "A multiscale model of adaptation and spatial vision for realistic image display," in *SIGGRAPH 98 Conf. Proc., Computer Graphics Annu. Conference Series*, pp. 287–298, ACM (1998).
31. E. Reinhard, M. Stark, P. Shirley, and J. Ferwerda, "Photographic tone reproduction for digital images," in *Proc. SIGGRAPH2002*, pp. 267–277, ACM (2002).
32. L. Tao and V. K. Asari, "An integrated neighborhood dependent approach for nonlinear enhancement of color images," in *Proc. IEEE Computer Society International Conf. on Information Technology: Coding and Computing—ITCC 2004*, Vol. 2, pp. 138–139 (2004).
33. D. J. Jobson, Z. Rahman, G. A. Woodell, "Statistics of visual representation," *Proc. SPIE* **4736**, 25–35 (2002).



**Li Tao** received her BS and MS degrees in electronics and communication engineering from Sichuan University, Chengdu, China, in 1998 and 2001, respectively. She is currently pursuing her PhD degree in the Department of Electrical and Computer Engineering, Old Dominion University, Norfolk, Virginia. Her research interests include digital signal processing, digital image processing, and computer vision.



**Vijayan K. Asari** joined the Department of Electrical and Computer Engineering, Old Dominion University (ODU), Virginia, as an associate professor in August 2000. Dr. Asari received his BSc (Engg.) degree in electronics and communication engineering from the University of Kerala and his MTech and PhD degrees in electrical engineering from the Indian Institute of Technology, Madras. He has been an assistant professor in T.K.M. College of Engineering, University of Kerala, India. He was with the National University of Singapore from 1996 to 1998 and with the School of Computer Engineering at Nanyang Technological University, Singapore from 1998 to 2000. Dr. Asari directs the Computational Intelligence and Machine Vision Laboratory at ODU. His research activities are in signal processing, image processing, neural networks, and digital system architectures for application specific integrated circuits. Dr. Asari is a senior member of the IEEE.